

# Nonuniform Circular Array Synthesis for Low Side Lobe Level Using Dynamic Invasive Weeds Optimization

Elhadi Kenane<sup>1</sup>, Fadila Benmeddour<sup>1, \*</sup>, and Farid Djahli<sup>2</sup>

**Abstract**—The use of invasive weeds optimization in the synthesis of antenna arrays has become popular in the last few years. This optimization method is robust, simple and can be easily improved. Like other stochastic algorithms, IWO suffers from premature convergence and other drawbacks. To overcome these problems, a dynamic IWO is proposed and used for synthesizing two antenna array topologies (linear and circular array). This proposed method tries to achieve an optimal array pattern by acting on the amplitude excitation of elements in the nonuniform circular array and their positions on the array, to obtain an array pattern with deep nulls in some directions of interferences and low side lobe level. For the linear array, the nulls control can be achieved by acting on the relative amplitude excitation of each element in the array for an optimal inter-element spacing. This proposed method improves the performance greatly and allows to achieve a maximum reduction in side lobe level in band Nulls with an acceptable dynamic range ratio (DRR). To show the performance of the proposed method, for each topology, our results are compared to other results of the literature.

## 1. INTRODUCTION

Antenna arrays are widely used in the wireless telecommunication systems. Even if the linear arrays are used most, circular arrays are most recommended in omnidirectional applications such as radar applications where a  $360^\circ$  coverage space is necessary. In addition, the electronically scanned circular arrays present mechanical simplicity because it does not need a mechanical rotation.

Usually, these applications require some characteristics in the array pattern such as a narrow main lobe beamwidth, reduced sidelobe level (SLL) [1], nulls towards interferers [2], shaped beam [3–5], and sum-difference pattern [6]. To achieve the requirements in pattern characteristics, some array parameters must be adjusted. Among these parameters, one can cite current distribution (amplitude and/or phase) and inter-element spacing.

The synthesis of antenna array that gives a desired pattern by adjusting one of the array parameters is a nonlinear problem. Since several classical synthesis methods fall in local minima, many stochastic methods have been applied to solve the array synthesis problems, such as evolutionary algorithms [7], cuckoo search optimization [8], particle swarm optimization (PSO) [9], and grey wolf optimization (GWO) [10].

These numerical methods have been used for the synthesis of antenna arrays whatever their topologies. There are many topologies and types of antennas arrays used in electronics systems such as planar arrays [11, 12], random antenna arrays [13], irregular arrays [14], sparse arrays [15], and prefractal monopolar antennas [16].

The invasive weeds optimization (IWO) is a stochastic method inspired from plant colonization [17]. Due to its advantages and robustness over several analytical and stochastic methods, the IWO became

---

*Received 4 February 2021, Accepted 31 March 2021, Scheduled 3 April 2021*

\* Corresponding author: Fadila Benmeddour (fadila.benmeddour@univ-msila.dz).

<sup>1</sup> LGE Laboratory, Electronics Department, Mohamed Boudiaf University, M'sila, Algeria. <sup>2</sup> Electronics Department, University of Setif, Setif, Algeria.

popular in many engineering optimization problems. However, the conventional IWO algorithm has some drawbacks. The dispersion of the produced seeds is uniform, which may be not suitable for nonlinear optimization problems. To overcome the demerits of the conventional IWO, a novel dynamic IWO has been proposed and used in this paper for the antenna array synthesis problems. In IWO, the standard deviation has a considerable significant concept as it can play an important role in the searching performance of the IWO. Therefore, a mutation process will be applied to the calculation of standard deviation during the spatial dispersal process of produced seeds while keeping the mean at the parent plants. In the mutation process, if special conditions are achieved, the standard deviation would be re-initialized. To evaluate the efficacy of the proposed stochastic method, we present a fair comparison with other works where many examples are illustrated.

In this paper, the synthesis of two topologies, the linear array and circular one has been presented. Firstly, our goal was to achieve an array pattern with an improved null at the third null position of the reference array pattern (uniform linear array  $I_n = 1$  and  $d = \lambda/2$ ). The achieved pattern has low side lobe level (SLL) while maintaining the main beam beamwidth narrower or equal to that of its corresponding reference array pattern.

In the second part, our dynamic IWO has been used for the synthesis of circular antennas array. To achieve some desired characteristics in the array pattern, deep nulls will be imposed at some directions of the reference pattern. The circular array is synthesized by controlling some array parameters such as amplitude excitation  $a_n$  and position  $d_n$ . For each example, a comparison was done with similar results of the literature.

## 2. ANTENNA ARRAY THEORY

In this paper, an evolutionary optimization method, namely the dynamic invasive weeds (DIWO), has been proposed and used to minimize a suitable cost function and synthesize the antenna arrays.

To illustrate the robustness of the proposed algorithm, two synthesis problems will be considered. To decrease the mutual coupling effects, the distance between elements is fixed to  $0.5\lambda$  in both cases. The different array elements are assumed to be isotropic. The IWO is carried out in five runs of 50 iterations for each one.

### 2.1. Linear Array

The linear array of  $2N$  elements is assumed symmetric with regard to its center. The array factor  $AF$  can be expressed by:

$$AF(\theta) = 2 \sum_{n=1}^N I_n \cos(k(n-0.5)d(\cos\theta - \cos\theta_0)) \quad (1)$$

where  $k = 2\pi/\lambda$  and  $\lambda$  is the wavelength,  $N$  the number of elements on each side of the array,  $d$  the inter-element spacing,  $\theta$  the observation angle from the axis of the array,  $\theta_0$  the pointing angle of the main beam (at broadside  $\theta_0 = 90^\circ$ ), and  $I_n$  the current excitation of the  $n$ th element on each side of the array. Only the amplitude will be controlled during the optimization process, and the phase distribution is maintained constant and equal to zero.

In this part, the linear array synthesis is done considering three examples ( $2N = 12, 16,$  and  $20$  elements) which can provide an array pattern with deep null, on each side of the main beam, with an acceptable level of the sidelobes. The nulls are imposed at the second and the third null positions of the reference pattern (uniform excitation  $I_n = 1$  and inter-element spacing  $d = \lambda/2$ ). The expression of  $AF$  is used to obtain the amplitude excitations and the inter-element spacing  $d$  that impose nulls towards specified directions and reduce the SLL while keeping the beamwidth of the main lobe equal to that of the reference pattern. These requirements are imposed using the following fitness function [18].

$$CF_{ULA} = C_1 \frac{\left| \prod_{m=1}^{M_{nu}} AF(\theta = null_m) \right|}{|AF(\theta_0)|} + C_2 \sum_{k_b=1}^{K_b} H(k_b)(Q_{k_b} - \delta) + C_3(BW_c - BW_d) \quad (2)$$

where  $M_{nu}$  is the number of nulls on either side of the main beam. Generally, the number of nulls that can exist on the pattern of an array depends on many factors such as pattern geometry, number of

elements, inter-element distance, and method of feeding.  $AF(\theta_0)$  is the value of the array factor at the direction of the main beam. The second term of Equation (2) is used to minimize the SLL to a given threshold  $\delta$ .  $K_b$  denotes the number of peaks of sidelobes in the reference pattern;  $Q_{k_b}$  is the sidelobe level (in dB) achieved by the adjusted parameters ( $I_n$  and  $d$ ) at the  $k$ th peak; and  $\delta$  is the desired threshold of the side lobe level (in dB).  $H(k_b)$  is defined as:

$$H(k_b) = \begin{cases} 1, & (Q_{k_b} - \delta) > 0 \\ 0, & (Q_{k_b} - \delta) < 0 \end{cases} \quad (3)$$

The third term is introduced to keep the bandwidth narrower than that of the reference pattern (uniform excitation with  $d = \lambda/2$ ).  $BW_c$  and  $BW_d$  are, respectively, the calculated and desired beamwidths.  $C_1$ ,  $C_2$ , and  $C_3$  are the weight factors depending on the importance of each term.

As in [18], we try to achieve an array pattern with deep nulls in some directions where the value of  $C_1$  must be higher than the values of  $C_2$  and  $C_3$ . The value of the threshold  $\delta$  is taken similar to that of the corresponding reference pattern ( $I_n = 1$ ,  $d = \lambda/2$ ). To minimize the dynamic range ratio, another term, whose expression is given by [19], can be introduced in the cost function.

$$DRR = \frac{\max(I_n)}{\min(I_n)} \quad (4)$$

### 2.2. Circular Array

A circular array consists of an array of  $M$  elements arranged in a ring in the  $x$ - $y$  plane with an inter-element spacing  $d = \lambda/2$  along the periphery of a circle, as shown in Fig. 1. As in the linear array case, we will neglect mutual coupling and assume that the elements are isotropic so that the far field array pattern is equal to the array factor (the element radiation pattern  $g(\theta, \Phi) = 1$ ). We are interested in the array pattern in the plane  $\Phi = 0^\circ$ , known as the elevation (or vertical) plane.

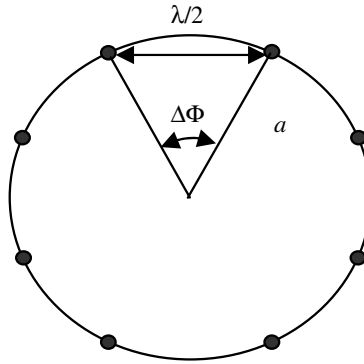


**Figure 1.** Geometry of a uniform circular array with  $M$  isotropic elements.

The array factor for this topology can be expressed as:

$$AF(\theta, \varphi) = \sum_{m=1}^M W_m \exp [-j \cdot k \cdot a \cdot (\sin \theta \cdot \cos (\varphi - \varphi_m)) - \sin \theta_0 \cdot \cos (\varphi_0 - \varphi_m)] \quad (5)$$

where

$W_m$  = amplitude excitation of the  $m$ th radiating element in the array.

$k = 2\pi/\lambda$  is the free-space propagation constant, and  $\lambda$  is the wavelength.

$a$  = the radius of the array.

$\theta_0$  = a vertical angle of the peak of the main beam direction.

$\varphi_0$  = a horizontal angle of the peak of the main beam direction.

$\varphi_m$  = an angular position of the  $m$ th element on  $x$ - $y$  plane.

After some simplifications, the following expression can be achieved:

$$AF(\theta, \varphi) = \sum_{m=1}^M W_m \cos \left[ k \cdot a \cdot \left( \sin \theta \cdot \cos(\varphi - \varphi_m) - \sin \theta_0 \cdot \cos \left( \begin{matrix} \varphi_m & - \varphi_m \\ 0 & \end{matrix} \right) \right) \right] \quad (6)$$

The cost function is the most important relationship between the synthesis problem and the stochastic method.

To minimize the average SLL, the cost function may therefore be expressed as:

$$CF1 = \sum_{i=1}^K \frac{1}{\Delta\varphi_i} \int_{\varphi_{Li}}^{\varphi_{Ui}} |AF^{\tilde{X}}(\varphi)|^2 d\varphi \quad (7)$$

$K$  is the number of regions ( $K = 2$ ),  $\Delta\varphi_i = \varphi_{Ui} - \varphi_{Li}$ , where  $\varphi_{Li}$  and  $\varphi_{Ui}$  are the lower and upper angles of the  $i$ th side, respectively.

In order to decrease the effect of the undesired interference signals, some nulls should be imposed at the specific directions using the following cost function:

$$CF2 = \sum_{k=1}^{M_{nu}} |AF^{\tilde{X}}(\varphi_{nuk})| \quad (8)$$

where  $M_{nu}$  is the number of nulls, and  $\varphi_{nuk}$  is the angle at the direction of the  $k$ th null.

A small side lobe, for a specific beamwidth, leads to high directivity. To reduce the SLL, the following fitness function must be minimized:

$$CF3 = \sum_{k=1}^K |AF^{\tilde{X}}(\varphi_{msk})| \quad (9)$$

$\varphi_{msk}$  is the angle which allows to reach the maximum side lobe level, in the  $k$ th region. In our study, the number of regions is fixed to two for all the examples.

Due to the size limitations in many applications, it is important to reduce the physical size (aperture) of the array antenna. The physical size of the circular array will be reduced by controlling its circumference as given in the following fitness function:

$$CF4 = \sum_{i=1}^N d_i \quad (10)$$

A tradeoff between physical size and mutual coupling effect has to be made. For this purpose, a minimum inter-element spacing must be considered.

The general form of the cost function used to obtain a desired pattern is given by:

$$CF\_NUCA = \alpha_1 CF1 + \alpha_2 CF2 + \alpha_3 CF3 + \alpha_4 CF4 \quad (11)$$

where  $\alpha_1$ ,  $\alpha_2$ ,  $\alpha_3$ , and  $\alpha_4$  are the weighting factors assigned to the fitness functions.

### 3. DYNAMIC INVASIVE WEEDS OPTIMIZATION

In this study, null control low SLL arrays are synthesized by using a dynamic IWO method. The flow of this method is similar to that of the traditional IWO [17], where we propose to change the conventional calculation of spatial dispersion by using some other hybrid processes. Our approach uses mutation process as in the genetic algorithm with a given probability of mutation. The application of this process allows a better exploration of the search space, which improves the obtained results.

The main phases of invasive weeds method are as follows:

- (1) Initially, a population of plants will be generated randomly in the search space.
- (2) Evaluation of each plant in the colony uses a cost function.
- (3) Reproduction of seeds, when each plant can produce a number of seeds according to its cost function as given in the following equation:

$$N_s(P_i) = integer \left[ ms + \left( \frac{M_s - ms}{BC - WC} \right) (C(P_i) - WC) \right] \tag{12}$$

where  $M_s$  and  $m_s$  are, respectively, the maximum and the minimum number of generated seeds by the plant  $P_i$ .  $BC, WC$ , and  $C(P_i)$  represent, respectively, the cost function (fitness) of the best plant, the cost function of the worst plant, and the cost function of the  $i$ th plant  $P_i$  within the colony.

- (4) Evaluation of spatial distribution of the produced seeds. These seeds will grow and will be added to the colony as new plants. This spatial distribution is given by:

$$SD(itr) = \left[ \frac{itr_{max} - itr}{itr_{max}} \right]^{mod} (SD_{ini} - SD_{fni}) + SD_{fni} \tag{13}$$

where  $itr_{max}$  is the maximum number of iterations, and  $itr$  is the actual iteration index.  $SD_{ini}$  and  $SD_{fni}$  denote respectively the initial and final standard deviation values, and  $mod$  represents the nonlinear modulation index, usually equal to 3 as in [20].

- (5) Dynamic mutation: unlike the classical IWO, spatial disperse is modified using a mutation process. Initially, a probability  $P_m$  is given. If  $P_m$  is less than a random value in the interval  $[0, 1]$ , the actual value of the standard deviation  $SD_{itr}$  will be replaced by its initial value  $SD_{ini}$ . Otherwise, the standard deviation  $SD_{itr}$  will be calculated using Eq. (13).

The proposed algorithm is as follows:

Step 1: A random number is generated.

Step 2: A fixed probability of mutation  $P_m$  is chosen.

Step 3: If the random number is greater than  $P_m$ , then

$SD_{itr} = SD_{ini}$ ;

Else

$SD_{itr}$  is calculated from Eq. (13).

Step 4: Repeat this algorithm for each iteration.

- (6) Limitation: if the number of plants in the colony achieves its maximum value ( $pop\_max$ ), we will keep just the  $pop\_max^{th}$  plants in the colony and discard the other plants.
- (7) Stop criteria: the phases (2) to (6) will be repeated until a maxim number of iterations is reached.

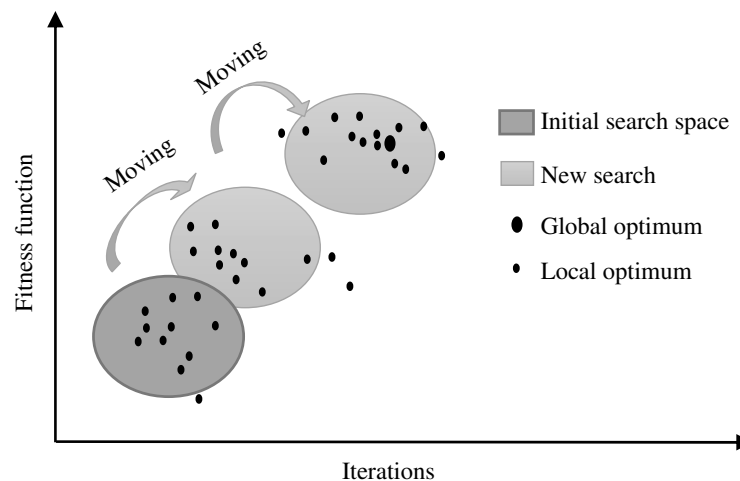


Figure 2. Dynamic IWO strategy.

The mutation rate is determined adaptively over each iteration. To avoid a premature convergence in a local minimum, a nonuniform mutation is used, in which the probability of mutation will be decreased iteratively as:

$$P_m(itr) = 1 - P_o \left(1 - \frac{itr}{itr_{max}}\right) \quad (14)$$

Note that the initial value of the mutation probability  $P_o$  is fixed to 0.8.

The mutation process makes the search space moving toward auspicious regions that may include the global optimum. This dynamic search space permits the IWO to increase the diversity of the plant colony with new solutions compared to the fixed search space (Fig. 2).

## 4. SIMULATION RESULTS

Dynamic IWO described in the previous section has been implemented to find the array weights (amplitude and/or phase) yielding an array pattern with some desired characteristics for both topologies cited previously.

### 4.1. Uniform Linear Array

In the first part of this study ( $2N = 12, 16,$  and  $20$  elements), dynamic IWO is used to find deep nulls imposed at the position of the third null of the reference pattern (uniform array:  $I_n = 1$  and  $d = \lambda/2$ ). The third null is placed at  $(\theta = 60^\circ, 120^\circ)$  for the first example and at  $(\theta = 68^\circ, 112^\circ)$  for the second example ( $2N = 16$ ), while the third null of the last example ( $2N = 20$ ) is imposed at  $(\theta = 72.5^\circ, 107.5^\circ)$ . The constraint is to reduce the SLLs and minimize the dynamic range ratio (DRR) while keeping the beamwidth close to that of the reference pattern. Here, the amplitude weights of current distribution along the array are controlled with an optimal inter-element spacing  $d$ . These amplitude weights can vary from 0 to 1, the current distribution is assumed symmetric, and  $d$  can vary from  $\lambda/2$  to  $\lambda$ . Each plant in the population is considered as a vector of the amplitude excitations and the inter-element spacing of the array elements. The problem dimension becomes  $(N + 1)$ , where the first  $N$  values represent the amplitude weights, and the  $(N + 1)$ th value represents the inter-element spacing.

Figures 3, 4, and 5 illustrate linear array patterns with an improved null at the third null for  $2N = 12, 16,$  and  $20$  elements, respectively. As can be seen, the optimized array patterns, for  $2N = 12, 16,$  and  $20$ , present an improved null, on each side of the main beam, at the third null position of

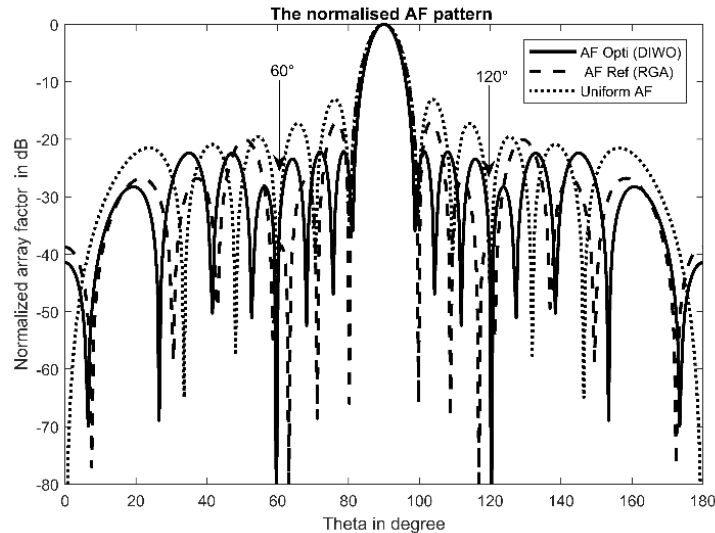


**Figure 3.** Comparison of different normalized array factors with excitation coefficients by DIWO (solid line), RGA (dashed line) and uniform array (dotted line) for  $2N = 12$ , nulls towards  $60^\circ$  and  $120^\circ$ .

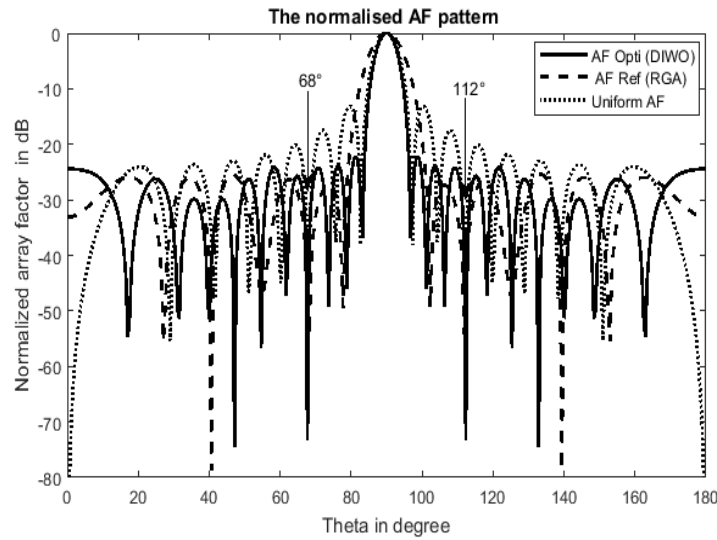


**Figure 4.** Comparison of normalized array factors with excitation coefficients by DIWO (solid line), RGA (dashed line) and uniform (dotted line) for  $2N = 16$  with an improved null imposed at the 3rd nulls ( $\theta = 68^\circ$  and  $\theta = 120^\circ$ ).

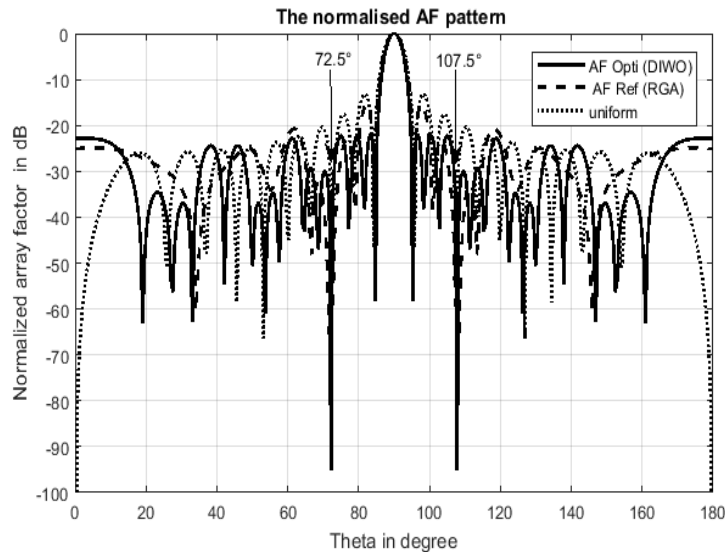


**Figure 5.** Comparison of normalized array factors with excitation coefficients by DIWO (solid line), RGA (dashed line) and uniform (dotted line) for  $2N = 20$  with an improved null imposed at the 3rd nulls ( $\theta = 72.5^\circ$  and  $\theta = 107.5^\circ$ ).

the corresponding uniform array pattern. The optimized array pattern using real genetic algorithm (RGA) [18] is shown in Figures 3, 4, and 5. Also, these figures illustrate a reduction in the maximum peak of the SLL (PSLL) with the obtained amplitude weights and the inter-element spacing, compared to that of the corresponding reference pattern ( $I_n = 1$  and  $d = \lambda/2$ ).

Table 1 shows some extracted characteristics from Figures 3, 4, and 5 such as peak SLL, beamwidth (first null beamwidth), and null depth. The DIWO pattern has a maximum SLL of  $-22.08$  dB for 12 elements,  $-22.13$  dB for 16 elements, and SLL of  $-21.98$  dB for 20 elements while RGA pattern has an SLL of  $-16.76$  dB for 12 elements, SLL of  $-25.39$  dB for 16 elements, and  $-15.46$  dB for 20 elements. We can note that the SLL is reduced by more than 6 dB compared to the SLL achieved by RGA for two examples ( $2N = 12$  and 20). For the second example, ( $2N = 16$ ), RGA presents the lowest SLL

**Table 1.** Pattern properties of a linear array for  $2N = 12, 16,$  and  $20$  elements (extracted from Figure 3, Figure 4, and Figure 5).

		uniform	RGA	DIWO
<b>12</b>	Null depth at 3rd null position in (dB)	-45.01	-54.75	<b>-87.41</b>
	Null direction in ( $^{\circ}$ )	60.20	58.66	<b>59.66</b>
	FNBW in ( $^{\circ}$ )	19.56	19.56	17.55
	PSLL (dB)	-13.05	-16.76	-22.08
<b>16</b>	Null depth at 3rd null position in (dB)	-40.10	-54.50	<b>-73.27</b>
	Null direction in ( $^{\circ}$ )	68.20	68.20	<b>67.70</b>
	FNBW in ( $^{\circ}$ )	14.54	24.54	<b>13.54</b>
	PSLL in (dB)	-13.13	-25.39	-22.13
<b>20</b>	Null depth at 3rd null position in (dB)	-40.60	-65.40	<b>-95.10</b>
	Null direction in ( $^{\circ}$ )	72.70	71.70	<b>72.20</b>
	FNBW in ( $^{\circ}$ )	11.54	11.54	<b>10.54</b>
	PSLL in (dB)	-13.16	-15.46	<b>-21.98</b>

**Table 2.** Excitation results for the linear array using the dynamic IWO method.

Number of elements		Optimal current excitation (normalized); $d$ in function of $\lambda$ DRR		
<b>12</b>	<b>RGA</b>	0.84511 0.6556 0.8444 0.71671 0.47139 0.40992; 0.58005	2.0616	
	<b>DIWO</b>	0.9744 0.9656 0.7586 0.6933 0.5235 0.4873; 0.6672	<b>1.9997</b>	
<b>16</b>	<b>RGA</b>	0.6013 0.5029 0.4866 0.4084 0.2438 0.1575 0.0173 0.0718; 0.5624	34.7572	
	<b>DIWO</b>	0.7216 0.7178 0.6641 0.5776 0.5358 0.4013 0.3668 0.3608; 0.6517	<b>2.0002</b>	
<b>20</b>	<b>RGA</b>	0.5478 0.7969 0.5051 0.5722 0.6221 0.6894 0.5206 0.4061 0.3769 0.1785; 0.6049	4.4644	
	<b>DIWO</b>	0.8808 0.8253 0.8584 0.8543 0.5667 0.6537 0.5398 0.5076 0.4471 0.4406; 0.6748	<b>1.9998</b>	

but with a big beamwidth. For the optimized array using RGA in [15], the achieved null depths are  $-54.75$  dB,  $-54.40$  dB, and  $-65.40$  dB, respectively, with a null direction towards  $58.68^{\circ}$  for  $2N = 12$  elements design,  $68.20^{\circ}$  for 16 elements design, and  $71.2^{\circ}$  for the last design problem.

For the first example ( $2N = 12$  elements with third null towards  $60^{\circ}$ ), the first null at the third null position ( $\theta = 60^{\circ}, 120^{\circ}$ ) is deeper than  $-87.41$  dB, and the second null imposed at the third peak ( $\theta = 68^{\circ}, 112^{\circ}$ ) is deeper than  $-3.27$  dB.

For each example, the optimized amplitude weights of current distribution with an optimal inter-element spacing obtained using the proposed DIWO as well as with another method (RGA) are illustrated in Table 2. For each case, the DRR is given to show the feasibility of the current distribution.

In the presented examples, the optimized current amplitudes obtained using our DIWO have the lowest DRR in comparison to those achieved using RGA as shown in Table 2.

The results depicted in Figures 3, 4, and 5 illustrate the robustness of the proposed DIWO in terms of deep nulls, narrow beamwidth, and reduced SLL.

For the second example ( $2N = 16$  elements), the SLL is reduced by more than 8 dB (from  $-13.13$  dB to  $-21.21$  dB) using DIWO.

To show better the effectiveness and the robustness of the proposed method, another example of  $2N = 20$  elements of linear array is synthesized. The optimized linear array must have an array pattern with a low side lobe level and two nulls imposed at the second and third peaks positions of the corresponding uniform linear array ( $I_n = 1$  and  $d = \lambda/2$ ). For this example, the nulls are imposed

**Table 3.** Pattern properties of a linear array for  $2N = 20$  elements (extracted from Figure 6).

$2N$			Uniform	RGA	DIWO
20	Null depth (dB)	2nd peak	-17.61	-71.00 (not towards the peak)	-66.5
		3rd peak	-20.40	-78.92 (not towards the peak)	-67.1
	FNBW in ( $^\circ$ )	-	11.54	11.96	12.36
	PSLL (dB)	-	-13.16	-13.85	-24.21

**Table 4.** Excitation results for the  $2N = 20$  elements linear array for nulls imposed at the second and third peaks using the dynamic IWO method.

Number of elements	Optimal current excitation (normalized); $d$ in function of $\lambda$							DRR	
20	RGA	0.6163	0.5076	0.7290	0.4194	0.7148	0.2845	0.8719	3.38
	DIWO	0.9747	0.9767	0.9679	0.8423	0.7220	0.6315	0.6866	
		0.4284	0.4281	0.4309	0.5865				<b>2.28</b>

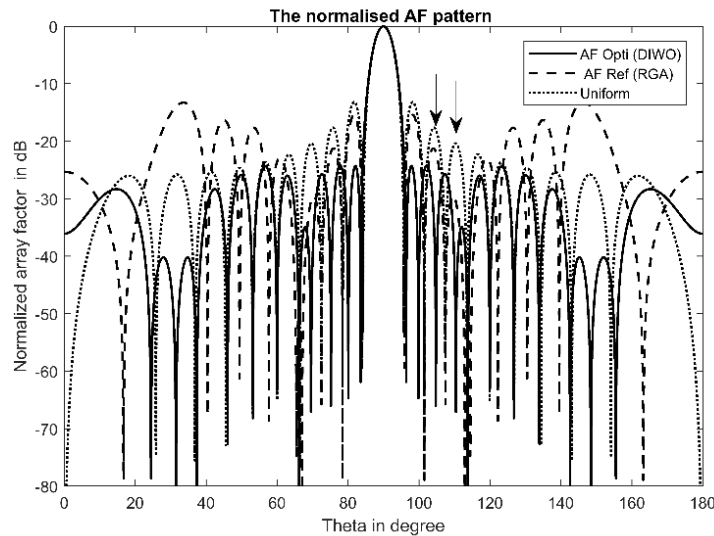


**Figure 6.** Comparison of normalized array patterns with excitation coefficients by DIWO (solid line), RGA (dashed line) and uniform (dotted line) for  $2N = 20$  with nulls imposed at the 2nd ( $\theta = 104.4^\circ$ ) and 3rd ( $\theta = 110.3^\circ$ ) peaks.

at the location of the second peak ( $\theta = 75.6^\circ, 104.4^\circ$ ) and at ( $\theta = 69.7^\circ, 110.3^\circ$ ) for the third peak location. The dynamic range ratio (DRR) is taken into account.

Figure 6 illustrates the array patterns for  $2N = 20$  elements with nulls imposed at the second peak ( $\theta = 75.6^\circ, 104.4^\circ$ ) and at the third peak ( $\theta = 69.7^\circ, 110.3^\circ$ ). As tabulated in Table 3, the first null at the location of the second peak is deeper than  $-66.5$  dB while the second null imposed at the location of the third peak is deeper than  $-67.1$  dB with a dynamic range ratio equal to 2.28 as indicated in Table 4.

## 4.2. Circular Array

In this last section, the dynamic IWO is applied to the design of circular arrays with different numbers of elements ( $M = 8, 10,$  and  $12$ ). The main goal of the synthesis problem is to achieve an array pattern having some desired characteristics by controlling element positions and amplitude excitations of the nonuniform circular array. The FNBW of uniform circular array having  $M$  equally spaced elements and uniform excitation is selected as a beamwidth reference. Table 5 illustrates some characteristics of the uniformly excited and equally spaced circular antenna array of  $M = 8, 10,$  and  $12$  elements.

**Table 5.** Initial value of SLL uniform circular array for  $I_n = 1$  and equally spaced  $d = 0.5\lambda$ .

N of Elements	SLL (dB)	HPBW ( $^\circ$ )	FNBW ( $^\circ$ )	$\sum d_i(\lambda)$
8	-4.170	32.32	69.98	4
10	-3.597	25.84	55.66	5
12	-7.165	21.52	46.22	6

In the first example, the circular array of  $M = 8$  elements is synthesized using our dynamic IWO to achieve an array pattern with low SLL and two deep nulls placed at  $-142^\circ$  and  $-72^\circ$  while keeping beamwidth equal to that of the reference pattern. The optimal positions and amplitude excitations are presented in Table 6. The optimal amplitude excitations using dynamic IWO have low DRR. The obtained array pattern is shown in Figure 7 in comparison to other array patterns obtained using IWO/WDO [22], FA [23], and COA [8].

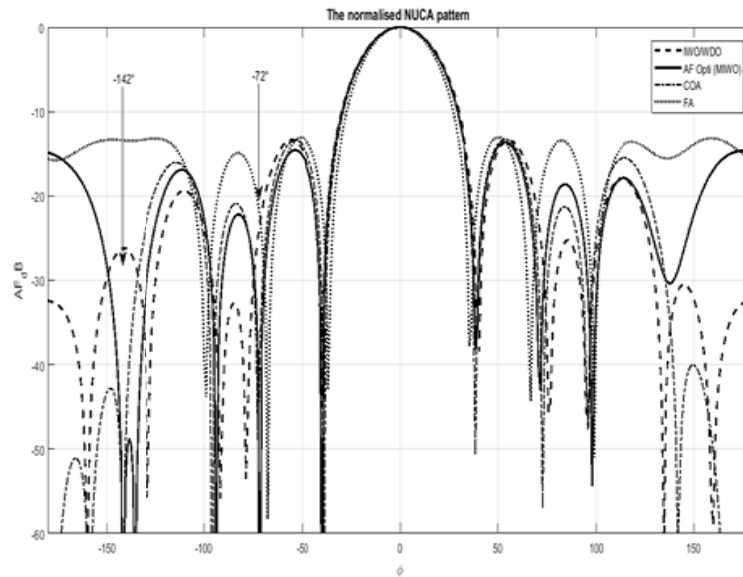


**Figure 7.** Normalized array patterns for NUCA, for  $M = 8$  elements using DIWO in comparison to other similar results.

**Table 6.** Position and amplitude of the nonuniform circular array, for  $M = 8$  elements using DIWO.

$N$	Position ( $d_n$ )	Excitation amplitude ( $a_n$ )
1	0.3095	0.8041
2	0.6661	0.1392
3	0.1328	0.3432
4	0.8116	0.8703
5	0.5772	0.9044
6	0.8221	0.4102
7	0.8453	0.8592
8	0.2934	0.1784

**Table 7.** Some characteristics of the NUCA, for  $M = 8$  elements using DIWO in comparison to other similar results.

Method	MSLL (dB)	ASLL (dB)	Null depth at		$\sum d_i(\lambda)$
			$-72^\circ$	$-142^\circ$	
<b>Hybrid IWO/WDO</b>	-13.52	-22.39	-23.8 dB	-26.20 dB	4.54
<b>GA</b>	-9.81	-13.70	-	-	4.40
<b>PSO</b>	-12.04	-20.31	-	-	4.43
<b>BBO</b>	-9.84	-15.96	-	-	4.58
<b>FA</b>	-12.93	-15.48	-22 dB	-14 dB	4.65
<b>CS</b>	-10.31	-17.09	-	-	4.46
<b>COA</b>	-13.32	-22.60	-49 dB	< -60 dB	4.44
<b>DIWO</b>	<b>-13.41</b>	<b>-20.61</b>	< -60 dB	< -60 dB	<b>4.46</b>

Some characteristics, extracted from the obtained array pattern, are compared with other similar results using reported stochastic methods in Table 7. The simulation results illustrate the performance of the proposed dynamic IWO compared to the other methods in terms of low SLL, deep nulls, and minimum circumference.

The obtained value of DRR (2.5357) using our dynamic IWO is better than the values achieved by other methods. Indeed, the obtained DRR using COA is 6.3638 with a circumference of  $4.44\lambda$  while the achieved circumference using the dynamic IWO is  $4.46\lambda$ , which is less than the circumference obtained by the method IWO/WDO ( $\sum d_i(\lambda) = 4.54\lambda$ ). In the other similar results shown in Table 7, the DRR is not taken into account.

In the second example, the dynamic IWO is used to synthesize a circular array of 10 elements. We consider here the same constraints as those used in the first example. Our goal is now to achieve an array pattern with low SLL and minimum circumference. As illustrated in Figure 8, the obtained array patterns using dynamic IWO, COA [8], GA [21], GWO [24] are compared with the corresponding uniform circular array pattern. These results clearly show the accuracy and performances of the proposed algorithm compared to other algorithms of the literature.

Table 8 presents the comparison between multiple results obtained using different stochastic methods, for the nonuniform circular array of 10 elements. These results show the optimal combinations (positions & amplitudes excitation) obtained by employing our dynamic IWO and the other results achieved by employing different stochastic methods in the literature for the same topology design. This table shows that our results, obtained with our DIWO algorithm, are largely better than the recently published results in terms of reduced DRR and minimization of circumference.

Table 9 shows that for obtained values of amplitude excitations and element positions using various stochastic methods, NUCA gives lower SLL response ( $-12.50$  dB) than UCA ( $-7.165$  dB) for same

**Table 8.** Position and amplitude of the nonuniform circular array, for  $M = 10$  elements using DIWO.

$\Phi_{nu2} = 27^\circ$	Position ( $d_n$ ) in $\lambda$ 's Excitation amplitude ( $a_n$ )
<b>GA</b>	[0.3641, 0.4512, 0.2750, 1.6373, 0.6902, 0.9415, 0.4657, 0.2898, 0.6456, 0.3282] $\Rightarrow$ <b><math>\Sigma dn = 6.0886</math></b>
	[0.9545 0.4283, 0.3392, 0.9074, 0.8086, 0.4533, 0.5634, 0.6015, 0.7045, 0.5948] $\Rightarrow$ <b>DRR = 2.8140</b>
<b>GWO</b>	[0.6808, 1.0277, 1.8984, 1.5751, 0.5528, 1.1361, 1.5082, 0.8024, 0.8502, 0.6082] $\Rightarrow$ <b><math>\Sigma dn = 10.6399</math></b>
	[0.3191, 0.3446, 0.2069, 0.5037, 0.4943, 0.1451, 0.2671, 0.0454, 0.3285, 0.4786] $\Rightarrow$ <b>DRR = 11.0947</b>
<b>COA</b>	[0.3214, 0.9695, 0.3671, 0.9672, 0.3232, 0.3194, 0.9681, 0.3662, 0.9703, 0.3233] $\Rightarrow$ <b><math>\Sigma dn = 5.8957</math></b>
	[0.5113, 0.2175, 0.4678, 0.4498, 0.7571, 0.7679, 0.5367, 0.5855, 0.5126, 0.6328] $\Rightarrow$ <b>DRR = 3.5306</b>
<b>PSO</b>	[0.3170, 0.9654, 0.3859, 0.9654, 0.3185, 0.3164, 0.9657, 0.3862, 0.9650, 0.3174] $\Rightarrow$ <b><math>\Sigma dn = 5.9029</math></b>
	[1.0000, 0.7529, 0.7519, 1.0000, 0.5062, 1.0000, 0.7501, 0.7524, 1.0000, 0.5067] $\Rightarrow$ <b>DRR = 1.9755</b>
<b>BBO</b>	[0.3870, 0.9088, 0.3232, 0.2549, 0.8932, 0.5083, 0.8781, 0.6733, 0.8800, 0.3498] $\Rightarrow$ <b><math>\Sigma dn = 6.0565</math></b>
	[0.8848, 0.5265, 0.3690, 0.3744, 1.0000, 1.0000, 0.6374, 0.5803, 0.8792, 0.5606] $\Rightarrow$ <b>DRR = 2.7100</b>
<b>FA</b>	[0.3810, 0.7453, 0.2668, 0.3142, 1.0000, 0.6032, 0.9706, 0.5713, 0.8800, 0.3376] $\Rightarrow$ <b><math>\Sigma dn = 6.0700</math></b>
	[0.7081, 0.2682, 0.3713, 0.4100, 0.8800, 0.9665, 0.4165, 0.5813, 0.7494, 0.5403] $\Rightarrow$ <b>DRR = 3.6037</b>
<b>DIWO</b>	[0.3338, 0.9336, 0.4010, 0.9806, 0.3355, 0.3373, 0.9930, 0.3710, 0.9663, 0.3303] $\Rightarrow$ <b><math>\Sigma dn = 5.9824</math></b>
	[0.5805, 0.2408, 0.4672, 0.5474, 0.6734, 0.7372, 0.5816, 0.4682, 0.6435, 0.6710] $\Rightarrow$ <b>DRR = 3.0614</b>

sizes. We also show that results obtained with our method are better than results obtained with other algorithms, in terms of low SLL, minimum DRR, and aperture size reduction. The obtained value of DRR, using our algorithm, is 3.06. Note that the array pattern obtained using GWO has the lowest SLL, but it has the highest DRR and the largest array aperture size.

In the last example, we have employed DIWO to synthesize a circular array of 12 elements. Figure 9 illustrates the optimal array pattern that has a maximum side lobe level of  $-15.13$  dB using DIWO method. The maximum SLLs achieved using the GWO, GA, PSO, BBO, FA, and COA are  $-17.37$ ,  $-11.83$ ,  $-13.67$ ,  $-14.37$ ,  $-14.21$ ,  $14.41$  dB, respectively.

Table 10 presents a comparison between results obtained using different stochastic methods, for a nonuniform circular array of 12 elements. This table shows well that the achieved results by employing our DIWO are better than the recently published results in terms of low SLL, reduced DRR, and minimization of circumference. The corresponding array patterns are presented in Figure 9.

In Table 11, the simulation results using the dynamic IWO are compared to those obtained using other stochastic methods such as COA, FA, PSO, and GWO. The comparison concerns the SLL, circumference, and DRR.

**Table 9.** Some characteristics of the NUCA for  $M = 10$  elements using DIWO in comparison to other similar results.

Method	MSLL (dB)	$\sum d_i(\lambda)$	DRR
<b>GWO</b>	-15.78	10.6399	11.0947
<b>GA</b>	-11.03	6.0800	2.8140
<b>PSO</b>	-12.30	<b>5.9029</b>	<b>1.9755</b>
<b>BBO</b>	-11.65	<b>6.0565</b>	<b>2.7100</b>
<b>FA</b>	-13.21	<b>6.0700</b>	<b>3.6037</b>
<b>CS</b>	-10.68	<b>5.7897</b>	NR
<b>COA</b>	-12.35	<b>5.8957</b>	<b>3.5306</b>
<b>DIWO</b>	<b>-12.50</b>	<b>5.9824</b>	<b>3.0614</b>

NR = Not Reported.

**Table 10.** Position and amplitude of the nonuniform circular array for  $M = 12$  elements using DIWO.

$\Phi_{nu2} = 23^\circ$	Position ( $d_n$ ) in $\lambda$ 's Excitation amplitude ( $a_n$ )
<b>GWO</b>	[0.5405, 1.1054, 0.6674, 1.3622, 1.1974, 0.4424, 0.4915, 1.0998, 1.3784, 0.7841, 1.0462, 0.5198] $\Rightarrow \Sigma dn = 10.6351$
	[0.1268, 0.0886, 0.0410, 0.0629, 0.1162, 0.1842, 0.1541, 0.0705, 0.0916, 0.0868, 0.1421, 0.2185] $\Rightarrow \text{DRR} = 5.3293$
<b>GA</b>	[0.4936, 0.4184, 1.4474, 0.7577, 0.4204, 0.5784, 0.4520, 0.8872, 0.7514, 0.4202, 0.4223, 0.7234] $\Rightarrow \Sigma dn = 7.7724$
	[0.2064, 0.5416, 0.2246, 0.6486, 0.7212, 0.7913, 0.5277, 0.3495, 0.5125, 0.4475, 0.5233, 0.8553] $\Rightarrow \text{DRR} = 4.1439$
<b>COA</b>	[0.2455, 0.8558, 0.6575, 0.6897, 0.8595, 0.3400, 0.1807, 0.8317, 0.6493, 0.7115, 0.8168, 0.2724] $\Rightarrow \Sigma dn = 7.1104$
	[0.9978, 0.6237, 0.5823, 0.7456, 0.9990, 0.9961, 0.5042, 0.6460, 0.6017, 0.6818, 0.9632, 0.7271] $\Rightarrow \text{DRR} = 1.9814$
<b>PSO</b>	[0.2569, 0.8509, 0.6607, 0.7057, 0.8540, 0.3734, 0.1609, 0.8321, 0.6464, 0.7079, 0.8330, 0.2682] $\Rightarrow \Sigma dn = 7.1501$
	[0.9554, 0.6441, 0.7109, 0.7769, 1.0000, 1.0000, 0.3958, 0.7162, 0.6746, 0.7695, 0.9398, 0.6145] $\Rightarrow \text{DRR} = 2.5265$
<b>BBO</b>	[0.4083, 0.6416, 0.7554, 0.7185, 0.6943, 0.3818, 0.3284, 0.8152, 0.9981, 0.3097, 0.7983, 0.3701] $\Rightarrow \Sigma dn = 7.2197$
	[0.6567, 0.3879, 0.6960, 0.4596, 0.5627, 0.9600, 0.4168, 0.5890, 0.5368, 0.6230, 0.6910, 1.0000] $\Rightarrow \text{DRR} = 2.5780$
<b>FA</b>	[0.3171, 0.8105, 0.5833, 0.7609, 0.8946, 0.4747, 0.9868, 0.2509, 0.2932, 0.7748, 0.6722, 0.3955] $\Rightarrow \Sigma dn = 7.2145$
	[0.9175, 0.3153, 0.5814, 0.6311, 0.9629, 0.9903, 0.3297, 0.4345, 0.6820, 0.4397, 0.7151, 0.7605] $\Rightarrow \text{DRR} = 3.1408$
<b>DIWO</b>	[0.2713, 0.8174, 0.5697, 0.7903, 0.9034, 0.4113, 0.1927, 0.8697, 0.5890, 0.6814, 0.7910, 0.3083] $\Rightarrow \Sigma dn = 7.1955$
	[0.8662, 0.6485, 0.4470, 0.6083, 0.9317, 0.9900, 0.4858, 0.6556, 0.5181, 0.5671, 0.9999, 0.6362] $\Rightarrow \text{DRR} = 2.2370$

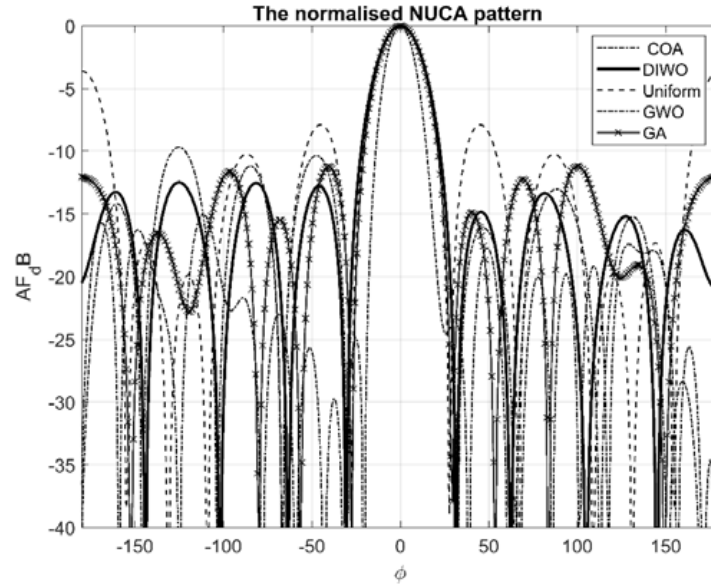


**Figure 8.** Normalized array patterns for NUCA, for  $M = 10$  elements using DIWO in comparison to other similar results.

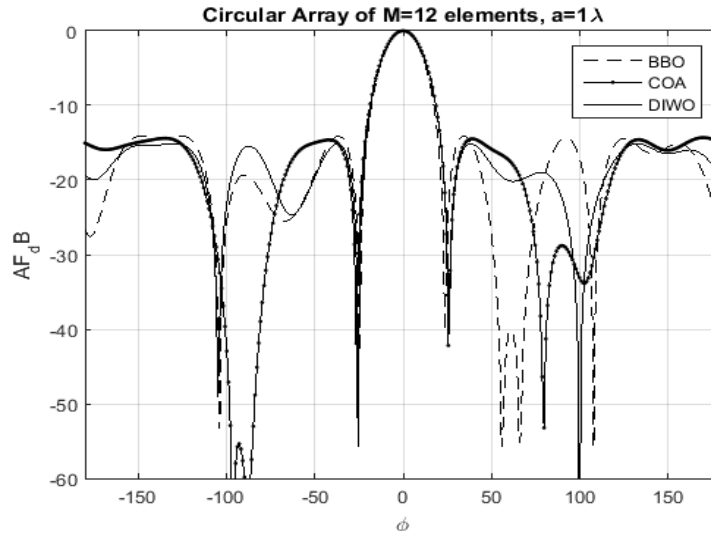


**Figure 9.** Normalized array patterns for NUCA, for  $M = 12$  elements using DIWO in comparison to other similar results.

**Table 11.** Some characteristics of the NUCA for  $M = 12$  elements using DIWO in comparison to other similar results.

Method	MSLL (dB)	$\sum d_i(\lambda)$	DRR
GWO	-17.37	<b>10.6351</b>	5.3293
GA	-11.83	<b>7.7724</b>	4.1439
PSO	-13.67	7.1501	2.5265
BBO	-14.37	<b>7.2197</b>	<b>2.5780</b>
FA	-14.21	<b>7.2145</b>	<b>3.1408</b>
COA	-14.41	<b>7.1104</b>	<b>1.9814</b>
DIWO	-15.13	<b>7.1955</b>	<b>2.2370</b>

From the above circular array examples, it can be seen that the results obtained using our dynamic IWO have the best combination of performance in terms of minimum circumference, reduced DRR, and low SLL. This effectiveness makes the DIWO competitive with other stochastic methods and very useful for antenna synthesis problem.

## 5. CONCLUSION

In this paper, a dynamic IWO was presented and successfully applied to the synthesis of two antenna array topologies (uniform linear array (ULA) and nonuniform circular array antenna (NUCA)). Moreover, the mutation process was used in the determination of the spatial dispersion ( $SD$  value) which allowed a good exploration of the search space and escaping from falling in local minima. In consequence, the convergence has been accelerated. For the first synthesis problem, the dynamic IWO was used to find excitation current amplitudes of ULA elements leaving the phase unmodified. For NUCA synthesis problem, positions and excitation amplitude were optimized to place deep nulls, minimize SLL, and reduce physical size of the array. For both arrays, the dynamic range ratio was also taken into account. Many simulation examples are illustrated, and the obtained results using dynamic IWO are compared with data from reference arrays and with RGA for the linear array and other stochastic methods for the optimized circular arrays such as COA, FA, and GWO. The achieved results show the robustness and performance of the dynamic IWO in terms of deep nulls, minimum SLL, low DRR, and physical size reduction.

## ACKNOWLEDGMENT

This work was supported by the Algerian Ministry of Higher Education and Scientific Research, Republic of Algeria, via funding through the PRFU project No. A25N01UN280120190001.

## REFERENCES

1. Dib, N., "Design of planar concentric circular antenna arrays with reduced side lobe level using symbiotic organisms search," *Neural Comput. Appl.*, Vol. 30, No. 12, 3859–3868, 2018.
2. Rahman, S. U., Q. Cao, M. M. Ahmed, and H. Khalil, "Analysis of linear antenna array for minimum side lobe level, half power beamwidth, and nulls control using PSO," *J. Microwaves, Optoelectron. Electromagn.*, Vol. 16, No. 2, 577–591, 2017.
3. Bai, J., Y. Liu, J. Cheng, P. You, and Q. Liu, "Shaped power pattern antenna array synthesis with reduction of dynamic range ratio," *2016 Progress In Electromagnetic Research Symposium (PIERS)*, 2444–2447, Shanghai, China, Aug. 8–11, 2016.
4. Battaglia, G. M., G. G. Bellizzi, A. F. Morabito, G. Sorbello, and T. Isernia, "A general effective approach to the synthesis of shaped beams for arbitrary fixed-geometry arrays," *Journal of Electromagnetic Waves and Applications*, Vol. 33, No. 18, 2404–2422, 2019.
5. Buttazzoni, G., F. Babich, F. Vatta, and M. Comisso, "Geometrical synthesis of sparse antenna arrays using compressive sensing for 5G IoT applications," *Sensors*, Vol. 20, No. 350, 1–16, 2020.
6. Rocca, P., M. Donelli, G. Oliveri, F. Viani, and A. Massa, "Reconfigurable sum-difference pattern by means of parasitic elements for forward-looking monopulse radar," *IET Radar, Sonar Navig.*, Vol. 7, No. 7, 747–754, 2013.
7. Slowik, A. and H. Kwasnicka, "Evolutionary algorithms and their applications to engineering problems," *Neural. Comput. Appl.*, Vol. 32, No. 16, 12363–12379, 2020.
8. Singh, U. and M. Rattan, "Design of linear and circular antenna arrays using cuckoo optimization algorithm," *Progress In Electromagnetics Research C*, Vol. 46, 1–11, 2014.
9. Caorsi, S., M. Donelli, A. Lommi, and A. Massa, "Location and imaging of two-dimensional scatterers by using a particle swarm algorithm," *Journal of Electromagnetic Waves and Applications*, Vol. 18, No. 4, 481–494, 2004.

10. Saxena, P. and A. Kothari, "Optimal pattern synthesis of linear antenna array using grey wolf optimization algorithm," *Int. J. Antennas Propag.*, Vol. 2016, 1–11, 2016.
11. Donelli, M. and P. Febvre, "An inexpensive reconfigurable planar array for Wi-Fi applications," *Progress In Electromagnetics Research C*, Vol. 28, 71–81, 2012.
12. Donelli, M., T. Moriyama, and M. Manekiya, "A compact switched-beam planar antenna array for wireless sensors operating at Wi-Fi band," *Progress In Electromagnetics Research C*, Vol. 83, 137–145, 2018.
13. Liang, S., Z. Fang, G. Sun, Y. Liu, G. Qu, and Y. Zhang, "Sidelobe reductions of antenna arrays via an improved chicken swarm optimization approach," *IEEE Access*, Vol. 8, 37664–37683, 2020.
14. Bulatsyk, O. O. and N. N. Voitovich, "Complex zeros of solutions to the synthesis problem of irregular linear antenna array by amplitude radiation pattern," *2017 XXII<sup>nd</sup> International Seminar/Workshop on Direct and Inverse Problems of Electromagnetic and Acoustic Wave Theory (DIPED)*, 14–19, 2017.
15. Shi, W., Y. Li, L. Zhao, and X. Liu, "Controllable sparse antenna array for adaptive beamforming," *IEEE Access*, Vol. 7, 6412–6423, 2019.
16. Zeni, E., M. Donelli, A. Massa, G. Boato, and R. Azaro, "Design of a prefractal monopolar antenna for 3.4–3.6 GHz Wi-Max band portable devices," *IEEE Antennas Wirel. Propag. Lett.*, Vol. 5, No. 4, 116–119, 2006.
17. Mehrabian, A. R. and C. Lucas, "A novel numerical optimization algorithm inspired from weed colonization," *Ecol. Inform.*, Vol. 1, No. 4, 355–366, 2006.
18. Goswami, B., and D. Mandal, "A genetic algorithm for the level control of nulls and side lobes in linear antenna arrays," *J. King Saud Univ., Comp. & Info. Sci.*, Vol. 25, No. 2, 117–126, 2013.
19. Vescovo, R., "Reconfigurability and beam scanning with phase-only control for antenna arrays," *IEEE Trans. Antennas Propag.*, Vol. 56, No. 6, 1555–1566, 2008.
20. Basak, A., S. Pal, S. Das, and A. Abraham, "Circular antenna array synthesis with a differential invasive weed optimization algorithm," *Tenth International Conference on Hybrid Intelligent Systems, IEEE Conference*, 153–158, USA, 2010.
21. Panduro, M. A., A. L. Mendez, R. Dominguez, and G. Romero, "Design of non-uniform circular antenna arrays for side lobe reduction using the method of genetic algorithms," *Int. J. Electron. Commun. (AEÜ)*, Vol. 60, No. 10, 713–717, 2006.
22. Mahto, S. K. and A. Choubey, "A novel hybrid IWO/WDO algorithm for nulling pattern synthesis of uniformly spaced linear and non-uniform circular array antenna," *Int. J. Electron. Commun. (AEÜ)*, Vol. 70, No. 6, 750–756, 2016.
23. Sharaq, A. and N. I. Dib, "Circular antenna array synthesis using firefly algorithm," *The International Journal of RF and Microwave Computer-Aided Engineering*, Vol. 24, No. 2, 139–146, 2013.
24. Das, A., D. Mandal, and R. Kar, "An optimal circular antenna array design considering mutual coupling using heuristic approaches," *The International Journal of RF and Microwave Computer-Aided Engineering*, Vol. 30, No. 11, 2020.